

A Novel Approach to Monitor Nonstationary Dynamics in Physiological Signals: Application to Blood Pressure, Pulse Oximeter, and Respiratory Data

BUFAN YANG and KI H. CHON

Department of Biomedical Engineering, Worcester Polytechnic Institute, 100 Institute Road, Worcester, MA 01609, USA

(Received 23 February 2010; accepted 27 May 2010; published online 11 June 2010)

Associate Editor Berj L. Bardakjian oversaw the review of this article.

Abstract—We propose a parametric time-varying (TV) algorithm which utilizes sinusoids as the basis functions which are then projected onto sets of Legendre and Walsh functions for the purpose of monitoring nonstationary dynamics. The proposed algorithm is a general-purpose algorithm that has the potential to be widely applicable to various physiological signals, but is especially well-suited for tracking blood pressure (BP), pulse oximeter, and respiratory signals, as they all exhibit periodic oscillations with TV dynamics. The proposed algorithm's efficacy was verified using both simulation examples and application to experimental data from all of the above-mentioned sources. Our results show that the method can: (1) accurately monitor abrupt frequency changes even when the data are contaminated with significant noise, (2) accurately monitor the BP and pulse oximeter signals, and (3) provide accurate estimation of respiratory rates derived directly from pulse oximeter recordings.

Keywords—Pulse oximeter, Respiratory rate, Basis functions, Time-varying, Sinusoids, Optimal parameter search.

INTRODUCTION

We propose an algorithm for monitoring frequency changes in physiological signals. The algorithm is well-suited for monitoring both slow and abrupt frequency changes with minimal time delay. Such an algorithm has wide application in the field of vital signs monitoring. For example, it can be used to monitor blood pressure (BP) and pulse oximeter signals. In fact, our algorithm is especially well-suited for monitoring any signals that exhibit a sinusoidal or periodic behavior. In addition, the method can be used to provide respiratory rates directly from pulse oximeter signals. Acquiring accurate respiratory rates from a pulse oximeter is

important because this information allows us to characterize whether a low oxygen saturation reading is due to low breathing rates or is the result of other dangerous physiological conditions. The patient's comfort is also improved greatly by obtaining this additional information from the pulse oximeter without having to wear a separate device for respiratory rate measurement. Traditionally, respiratory rates are extracted from an ECG signal only by donning an additional device than the pulse oximeter.³ An additional clinical benefit is that respiratory rate information can be used as one of the parameters to detect the conditions leading to, and therefore prevent, sudden infant death syndrome in clinical settings.⁹ Furthermore, subjects with chronic heart failure (CHF) often develop various forms of oscillatory periodic breathing patterns. These patterns can be classified into ventilation with and without apnea.¹² The breathing pattern with apnea, which has the characteristics of sudden cessation of breathing followed by normal respiratory patterns, known as Cheyne-Stokes respiration (CSR), is especially prevalent among CHF subjects and can lead to increased mortality.² For those CHF subjects without apnea, breathing rates change slowly. Thus, for cases such as CSR and CHF subjects without apnea, it is desirable to have an algorithm that can monitor both sudden and slow changes in respiratory rates.

We have recently developed a non-model based time-frequency analysis to extract respiratory rates directly from pulse oximeter recordings and found excellent accuracy for breathing rates up to 36 breaths per minute.⁷ We have recently determined that the same time-frequency technique can also be directly applied to ECG recordings to obtain respiratory rates.⁷ An autoregressive (AR) model-based technique to extract breathing rates from pulse oximeter data has also been developed,¹¹ but we found that its accuracy

Address correspondence to Ki H. Chon, Department of Biomedical Engineering, Worcester Polytechnic Institute, 100 Institute Road, Worcester, MA 01609, USA. Electronic mail: kichon@wpi.edu

was not as good as the non-model based time–frequency approach.⁷ This compromise in accuracy with an AR model was largely due to its reliance on the Akaike information criterion for model order determination.¹⁵ However, the motivation for using an AR model approach over non-parametric time–frequency analysis is mainly due to the well-known fact that the former method’s accuracy is less dependent on the data length.²⁰ Thus, one of the motivations of our approach using sinusoidal basis functions in this work was to utilize an efficient AR model order criterion, known as the optimal parameter search (OPS), which has been shown to be accurate for time-invariant (TIV) and time-varying (TV) parametric models.^{27,29}

Most of the vital signs derived from the measured physiological signals are cyclical and exhibit sinusoidal characteristics. Thus, extraction of nonstationary frequencies in these signals necessitates representation of the measured data (e.g., BP or pulse oximeter) as a truncated TV Fourier series. Specifically, TV frequency components are determined by projecting them onto a set of orthogonal basis functions.²⁹ The benefit of such an approach is that it leads to a significant reduction in the number of parameters required to track TV frequencies. In addition, TV parameters become TIV, which allows the use of the least-squares approach to solve for the unknown coefficients. Finally, the use of basis functions facilitates tracking of both fast and slow changing frequencies by incorporating multiple basis functions, which are particularly well-suited for capturing diverse dynamics.⁶ For the purpose of monitoring physiological dynamics such as the respiration, BP, and pulse oximeter signals, our algorithm utilizes sinusoids as the basis functions and then the OPS algorithm is used to find only the significant frequency terms that best characterize the dynamics of the data. Only those chosen significant frequency terms are then projected onto sets of Legendre and Walsh functions for tracking slow and fast nonstationary dynamics, respectively.

We demonstrate our robust frequency monitoring algorithm using both simulation examples and application to diverse physiological signals. The applications include tracking of BP and pulse oximeter signals, and extraction of respiratory rates from pulse oximeter recordings.

METHODS

Algorithm Description

The algorithm utilized is the OPS, a method developed in our laboratory.¹⁹ The OPS has been shown to be an accurate method for automatic model order selection and results in robust parameter estimation for

linear and nonlinear AR moving average models.¹⁹ In this work, we use the OPS to obtain coefficient estimates of the sinusoidal series. Thus, the proposed method will be referred to as TVSINCOS henceforth.

A TV time series can be described by a polynomial of the form.⁵

$$y(n) = \sum_{m=1}^M a_{m,n} P_m(n) + e(n), \quad (1)$$

where $P_m(n)$ are basis functions and M is the total number of basis functions. The $a_{m,n}$ are the TV coefficients and $e(n)$ is a noise source. The basis functions are chosen from the sinusoidal series such that

$$P_1(n) = \cos(\omega_1 n) \quad \text{and} \quad P_2(n) = \sin(\omega_1 n) \quad (2)$$

More generally, for $i = 1, 2, \dots$

$$P_{2i-1}(n) = \cos(\omega_i n) \quad \text{and} \quad P_{2i}(n) = \sin(\omega_i n) \quad (3)$$

We have chosen the basis functions to be sinusoidal series since the aim is to track oscillatory characteristics of the BP and photoplethysmograph (PPG) signals. Substituting (3) into (1) gives

$$y(n) = \sum_{i=1}^{M/2} [b_{i,n} \cos(\omega_i n) + c_{i,n} \sin(\omega_i n)] + e(n) \quad (4)$$

The $b_{i,n}$ and $c_{i,n}$ are the cosine and sine amplitudes, respectively, and they represent the $a_{m,n}$ terms in Eq. (1). Note that M corresponds to the maximum number of sine and cosine functions. To track TV frequencies of the BP and PPG signals, we project them onto multiple sets of basis functions. Specifically, we use both Legendre and Walsh functions (all represented as $\pi_k(n)$) as we have shown previously that they are especially well-suited for tracking slow and fast dynamics, respectively.⁶ As shown in Fig. 1, Walsh functions should be used when the dynamics exhibit fast transients and burst-like characteristics, whereas Legendre polynomials are more appropriate for smoothly changing dynamics. Most physiological signals exhibit both fast and slowly varying dynamics at varying stages of the signal, thus, having both Legendre and Walsh basis functions alleviates having to make the decision *a priori* of which basis function is more appropriate for a particular signal. With this projection of TV parameters onto multiple sets of basis functions, Eq. (4) can be rewritten as:

$$y(n) = \sum_{i=1}^{M/2} \sum_{k=0}^V [\alpha(i, k) \pi_k(n) \cos_i(n) + \beta(i, k) \pi_k(n) \sin_i(n)] + e(n), \quad (5)$$

where $\alpha(i, k)$ and $\beta(i, k)$ represent the expansion parameters with V as the maximum number of basis

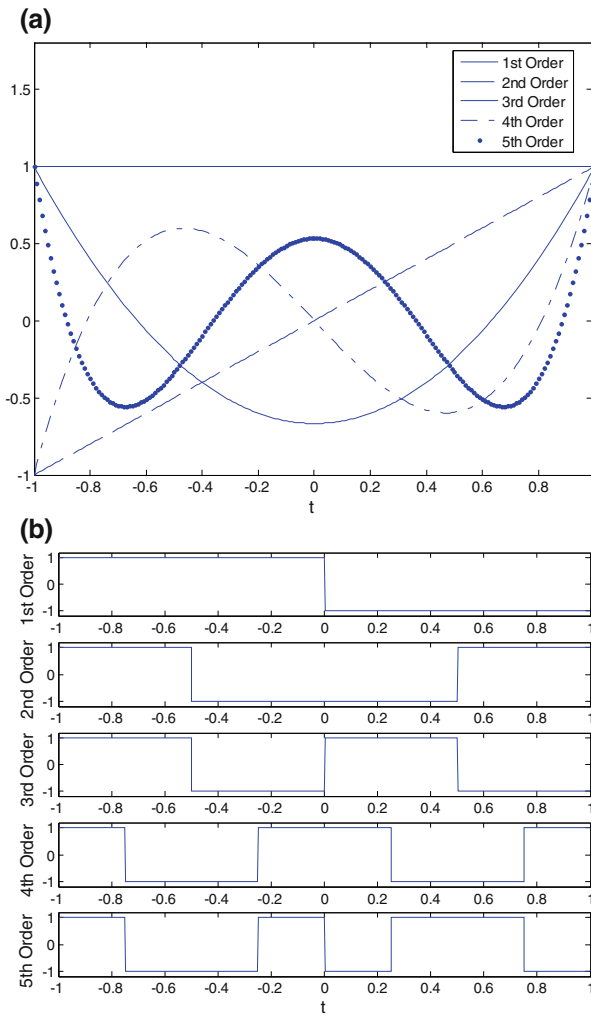


FIGURE 1. Dynamic characteristics of the first five order of Legendre (a) and Walsh (b) functions.

sequences. Once the multiple basis functions (Legendre and Walsh in our application) $\pi_k(n)$ have been chosen based on the normalized mean square error (NMSE) criterion (as discussed in the [Discussion and Conclusion](#) section), we denote a new set of TV sinusoidal functions as:

$$\begin{aligned} \cos_{i,k}(n) &= \pi_k(n) \cos_i(n) \\ \sin_{i,k}(n) &= \pi_k(n) \sin_i(n) \end{aligned} \quad (6)$$

Substituting (6) into (5) yields the equation:

$$y(n) = \sum_{i=1}^{M/2} \sum_{k=0}^Y [\alpha(i,k) \cos_{i,k}(n) + \beta(i,k) \sin_{i,k}(n)] + e(n), \quad (7)$$

where $\alpha(i,k)$ and $\beta(i,k)$ are TIV since they are not functions of discrete time, n . Given Eq. (7), the next step is to use the OPS algorithm to estimate the

unknown coefficients using the least squares. The advantage of the OPS is that it provides accurate parameter estimates because it is able to discriminate only the significant model terms among many candidate terms.

The first step of the OPS is to select linearly independent vectors among all initial candidates to form a new candidate vector pool. Let $\Phi = [w_0, w_1, \dots, w_R]$ denote the new pool, where R is the total number of selected linearly independent vectors. Once all linearly independent vectors have been selected, least-squares analysis is performed on the following equation:

$$y(n) = \Phi \theta_m^T + e(n), \quad (8)$$

where

$$\theta_m = [g_0, g_1, \dots, g_R], \quad \text{and} \quad \Phi = [w_0, w_1, \dots, w_R].$$

g_i is the coefficient estimate of the model and the objective now is to minimize the equation error $e(n)$. To minimize the error in Eq. (8), the cost function in Eq. (9) is used and parameter estimates can be made according to Eq. (10).

$$J_N(\theta_m) = [y(n) - \Phi \theta_m^T]^2. \quad (9)$$

$$\hat{\theta}_m = [\Phi \Phi^T]^{-1} \Phi y(n) \quad (10)$$

The projection distance is calculated as:

$$c_m = \frac{1}{N} \sum_{n=1}^N \hat{\theta}_m^2 w_m(n)^2, \quad m = 1, \dots, R. \quad (11)$$

With an initial model order of p_{ini} , the significant model order p_{opt} is determined by the ratio of two neighboring projection distances²⁹ described as:

$$p_{\text{opt}} = \arg \max_{m \in \{1, \dots, p_{\text{ini}}\}} \left(\frac{c_{m-1} - c_m}{c_m} \cdot 100 \geq \tau_{\text{th}} \right), \quad (12)$$

where c_m is the m th longest projection distance and τ_{th} is a threshold percentage. We have shown that a τ_{th} value of 25 works well in most cases.^{19,29} Thus, it is an effective model order search algorithm that has been shown to be more accurate than the Akaike Information criterion, minimum description length and the fast orthogonal search approaches.¹⁹ Further details regarding the OPS can be found in reference 21.

Simulation Examples

One of the key applications of the algorithm is to extract breathing rates from pulse oximeter recordings.^{1,7,11} Thus, we provide results from simulation examples in this section and actual extraction of human respiratory rates from a pulse oximeter in the subsequent section.

Simulation Example 1

The first simulation example was designed to examine the capability of our algorithm to detect sudden changes in frequencies. We generated the following 1200 data point time series (equivalent to 1 min at a 20 Hz sampling rate) with two frequencies of 0.4 and 0.3 Hz, where only the 0.4 Hz portion of the signal operates during the first 600 data points, and for the remaining portion of the data, only 0.3 Hz is present:

$$y(n) = A(n) \cos\left(2\pi f(n) \frac{n}{f_s} + \phi\right), \quad (13)$$

where $A(n)$ represents the amplitude, and ϕ and f_s denote the phase and sampling rate, respectively. To the time-series, $y(n)$, a 10 dB Gaussian white noise (GWN) was added. The candidate terms searched consisted of 20 frequencies ranging from 0.1 to 1.9 Hz at an increment of 0.1 Hz. We used five Walsh functions for this example based on the use of the mean square criterion as detailed in our previous work.¹⁵

Simulation Example 2

To demonstrate the TVSINCOS ability to extract respiratory rates, we performed a second simulation involving the following model:

$$y(n) = A_h(n) \cos\left(2\pi f_h(n) \frac{n}{f_s} + \phi_h\right) + A_b(n) \cos\left(2\pi f_b(n) \frac{n}{f_s} + \phi_b\right), \quad (14)$$

where subscripts h and b represent the heart rate and breathing components, respectively. The notations A and f_s represent the signal magnitude and sampling frequency, respectively, and ϕ is a random phase. We generated two series, each consisting of 600 data points with a sampling rate of 20 Hz, which provides sufficient resolution for resolving respiratory rates for both experimental and simulation data.⁷ For the first series, f_h and f_b were set to 1 and 0.4 Hz, respectively, while for the second series, they were set to 1.4 and 0.3 Hz. The higher frequency denotes the heart rate while the lower frequency represents the respiratory rate. The magnitude associated with the higher frequency is 10 times greater than the slow signal in Eq. (14). The above two series represent a TIV model. To represent a TV signal, we spliced together the two series as indicated above to yield a 1200 data points (1 min equivalent). Further, we added 10 dB GWN of equal data length to the spliced output time series. The candidate frequencies searched consisted of 20 frequencies ranging from 0.1 to 1.9 Hz at an increment of 0.1 Hz. For

TIV time series, Legendre and Walsh functions were not used, and TVSINCOS models, only one Walsh function was utilized. Our choice of one Walsh function is based on the design of the simulation example where breathing rates not only change from one time segment to the next, but also change abruptly. However, it should be noted that our simulation example is not unrealistic as CSR does have sudden changes in breathing patterns. Further, we assume that there cannot be more than one breathing rate from one time segment to the next. With the OPS, the eight most significant frequency terms were selected for both time series to ensure that both TIV and TVSINCOS models have the same model structure. Estimation errors were compared via the t test.

Data Acquisition

Pulse Oximeter Data

Data were collected from 15 healthy subjects (seven female and eight male, mean age 21 ± 1.2 years) and none had any cardiorespiratory pathologies. We used an MP506 pulse oximeter (Nellcor Oximax, Boulder, CO) reusable sensor (Durasensor DS-100A), which contained a conditioning circuit and has an analog output of 4.864 kHz. Data were collected in the supine position, and the pulse oximeter sensor was attached to the subjects' left index or middle finger. The subjects were instructed to breathe at a constant rate according to a timed beeping sound, i.e., to start an inspiration whenever they heard a beep sound programmed at a chosen frequency. The data were collected for breathing frequencies ranging from 0.2 to 0.6 Hz at an increment of 0.1 Hz. Before 3 min of data were collected for each frequency, subjects were allowed to practice breathing at the beeping rate. We also obtained the true breathing signal as a reference, via the Resptrace system which uses inductive plethysmography to provide calibrated voltage outputs corresponding to rib cage and abdominal compartment volume changes. The Resptrace system is cumbersome to use since inductive bands are worn over the rib cage and abdomen, and the system requires calibration for each subject and is more expensive than a pulse oximeter. Since in this study we are merely interested in the rate of respiration and not the amplitude, a simple FFT and/or manual counting of the number of peaks can be done on the Resptrace signal to obtain the frequency of oscillation. Data acquisition was done using the ADInstruments PowerLab/4Sp data acquisition system and routed into the PC via a universal serial bus (USB) port. Chart v4.2.2 software (ADInstruments, Colorado Springs, CO) was used to sample the analog signal at 200 Hz.

Blood Pressure Data

Ten healthy volunteers—five male and five female—were studied [age, $25.2 + 3.7$ years (mean + SD)]. All subjects were non-smokers and none took any medication. Written informed consent was obtained from all participants and the experimental protocol was approved by the Worcester Polytechnic Institute's committee on the use of humans as experimental subjects. Finger arterial pressure was recorded continuously (2300 Fingapres BP monitor, Ohmeda, Madison, WI, USA) from subjects in the supine position. Arterial BP obtained by this method has been shown to be in good accordance with central and intra-arterial pressure in various situations.²³

Experimental Data Analysis

Monitoring PPG and BP Signals

For the tracking of pulse oximeter and BP signals, we selected 3 min of data sampled at 200 Hz, which were then down-sampled to 20 Hz. For both data sets, the candidate sinusoidal frequencies to be searched were initially set to a wide frequency range, 0.1–3.5 Hz, at an increment of 0.1 Hz. We used four Legendre and 11 Walsh functions for the pulse oximeter data, whereas four Legendre and 15 Walsh functions were utilized for all BP signals. The NMSEs were calculated for varying combinations of basis functions and among them we selected the one with the lowest value. Further, we report averaged NMSE values for the training and testing data sets for all results including the simulation example. The training and testing data were based on the first and last half of the data for the experimental data, respectively. Among 35 candidate frequencies, only the 15 and 20 most significant candidate terms as determined by Eq. (12) of the OPS method for the pulse oximeter and BP data, respectively.

Respiratory Rate Estimation from PPG

The second task was to extract respiratory rates from the above-described pulse oximeter recordings using our proposed approach. Data analysis was performed on a 1 min segment (equivalent to 1200 data points) which was then shifted by 10 s for the entire 3 min recording for each breathing frequency (0.2–0.6 Hz) data set. Thus, near real-time updates of respiratory rates were provided. We used the NMSE as a means to quantify the tracking capability of our algorithm. All results are provided as mean \pm SD. Given our *a priori* knowledge that breathing frequencies ranged from 0.2 to 0.6 Hz at an increment of 0.1 Hz, we limited our candidate frequencies to be

searched from 0.1 to 0.8 Hz at an increment of 0.05 Hz. We used four Legendre and 11 Walsh functions and among 15 candidates, the OPS selected the 10 most significant frequencies. Note that for a chosen frequency, there might be both sine and cosine basis functions associated with it. Thus, the respiratory rate was chosen by selecting the most common frequency among 130 frequencies (10 significant terms among 13 segments). The results were then averaged for each breathing rate for all 15 subjects.

RESULTS

Simulation 1 Results

The task for this simulation example was to examine if our proposed method is able to capture TV frequencies of 0.4 and 0.3 Hz, where the former and latter frequencies appear only for the first and second half of the signal, respectively. To make the example more challenging, we have added 10 dB GWN. Among 20 candidate frequencies, the use of OPS led to the selection of only four significant frequency terms. Figure 2 shows the tracking capability of our proposed method. As shown, the four candidate terms are related to the 0.4 and 0.3 Hz. In the first half of the signal, both 0.4 and 0.3 Hz are chosen, but the magnitude associated with 0.4 Hz is significantly large whereas for 0.3 Hz, its magnitude is near zero. Thus, we can conclude that only the 0.4 Hz appears in the first half of the signal. Similarly, the same observation holds for the 0.3 Hz in the second half of the signal.

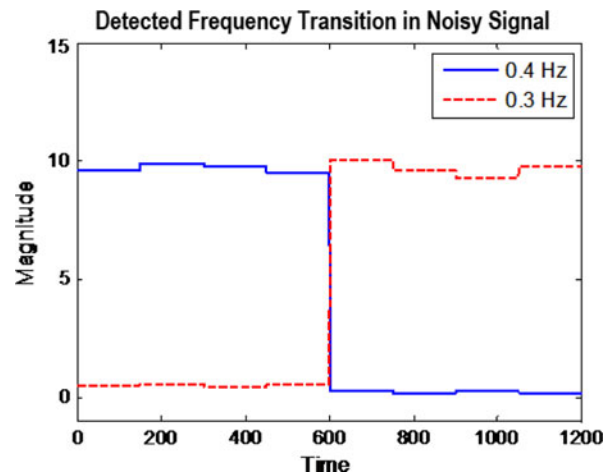


FIGURE 2. Large magnitude values associated with 0.4 Hz as compared to 0.3 Hz during the first half of the data signifies only the 0.4 Hz is present and vice versa during the second half of the data. The result is based on data corrupted by 10 dB additive noise.

Simulation 2 Results

The task of the second simulation example was to examine the efficacy of the proposed method in monitoring a signal that mimicks dynamics of the heart rate which is modulated by respiration. Figure 3a shows a representative nonstationary signal generated via Eq. (14) which was corrupted by 10 dB additive GWN (solid line) and the estimated time series (dotted line) via our TVSINCOS approach. Figures 3b and 3c represents a small portion of the signals shown in Fig. 3a using our TVSINCOS and TIV approaches, respectively. As expected, our TVSINCOS method is better able to track the signal than its TIV counterpart. Note that while our TVSINCOS method tracks the noise-corrupted signal reasonably well, it is not able to capture every change of the peak and valley magnitudes of the signal. However, this is the desired outcome since the algorithm should only track the clean portion of the signal and not the noise-corrupted data.

Thus, in Fig. 3d, we show the noiseless (solid line), TVSINCOS (dotted line), and TIV (dashed line) estimated signals. In this plot, we are not able to discern the differences between the noiseless and TV estimated signals as they are nearly identical, indicating that our algorithm is able to track accurately the clean portion of the signal. The NMSE values for TVSINCOS and TIV approaches for this representative data are 16.49 and 58.25%, respectively, for the noise-corrupted signal. The averaged NMSE values for the training and testing data sets are shown in Table 1. We also show in Table 1 that the averaged NMSE values obtained by the TV autoregressive model (TVAR), which utilizes the OPS for model order selection. The only difference between TVAR and the TVSINCOS is that the $P_m(n)$ terms in Eq. (1) are a function of past values of the signal itself rather than sine and cosine functions, respectively. Note that TVSINCOS is significantly more accurate than both TIV and TVAR approaches

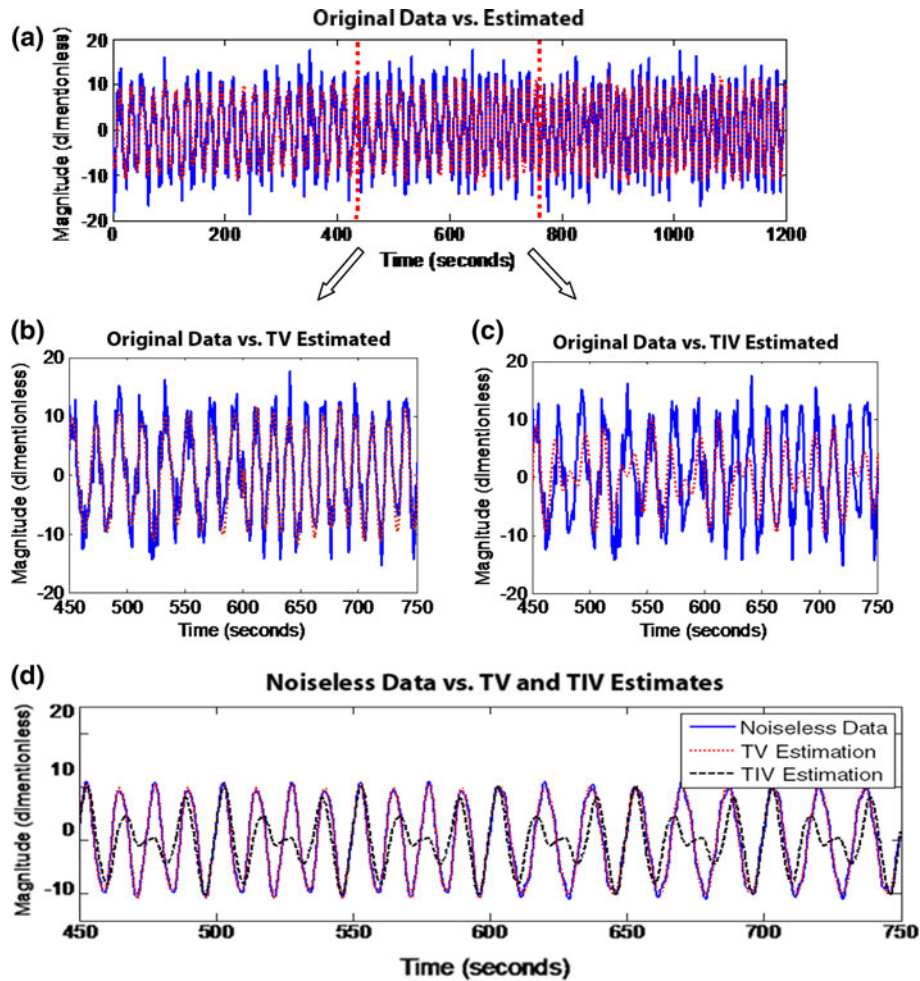


FIGURE 3. (a), (b), (c) show the comparison of TV and TIV method on 10 dB noise-corrupted data, (d) is estimation on clean signal which illustrates that our approach tracks the real signal instead of noise, note that the first 600 points have different frequencies to the second half.

TABLE 1. NMSE comparison between three different approaches for the simulation example, blood pressure and pulse oximeter data.

Methods	NMSE values (%)	
	Training	Testing
Simulation examples		
TVSINCOS	15.33 ± 2.74	16.23 ± 3.13
TIV	60.83 ± 3.80	63.93 ± 4.77
TVAR	23.18 ± 2.05	24.91 ± 2.96
Blood pressure data		
TVSINCOS	13.97 ± 2.73	15.35 ± 2.63
TIV	80.24 ± 3.40	79.66 ± 4.15
TVAR	17.34 ± 2.71	19.98 ± 3.07
Pulse oximeter data		
TVSINCOS	5.47 ± 1.39	6.26 ± 1.25
TIV	78.55 ± 4.55	83.55 ± 4.19 *
TVAR	6.45 ± 1.45	7.01 ± 1.07

*Denotes statistical significance between training and testing data ($p < 0.05$).

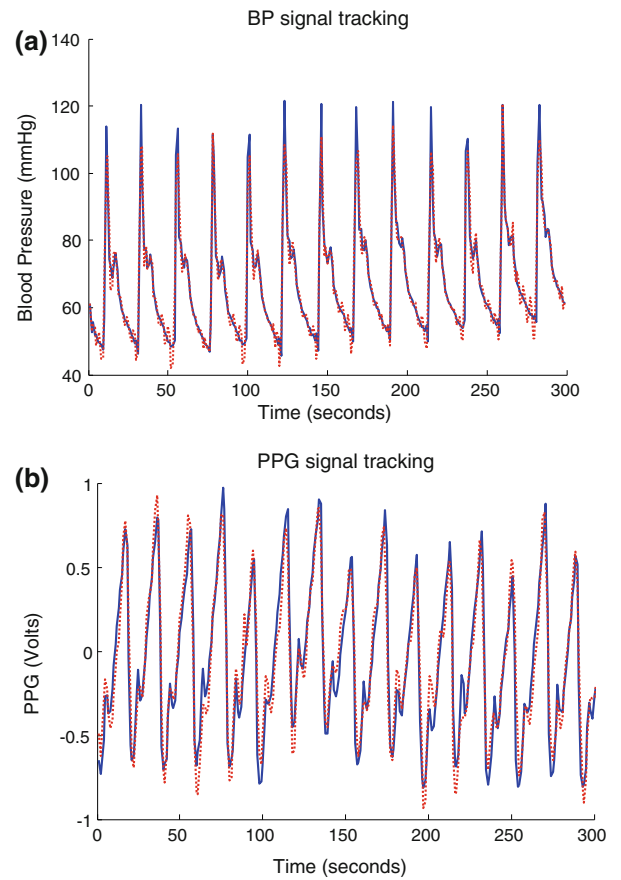
TABLE 2. Appearance of model frequency terms.

True frequency terms (Hz)	# Of times (%) selected
0.3	100
0.4	100
1.0	95
1.4	100

even though the total number of the parameters used was the same for TVAR and TVSINCOS. Further, our TVSINCOS algorithm is able to detect all four frequencies used to generate the time series of Eq. (14) (1, 0.4, 1.4, and 0.3 Hz) despite significant noise contamination. Table 2 shows the occurrence of the most frequently represented frequency terms based on 100 realizations.

Application of the Method for Tracking the Blood Pressure and Pulse Oximeter Data

Figures 4a and 4b shows representative BP and pulse oximeter signals (solid lines), respectively; superimposed are the TV estimated signals (dotted lines). Both BP and pulse oximeter oscillations are well-characterized by our TV approach albeit the tracking capability is better for the latter signal. The NMSE values are 14% for BP and 5% for pulse oximeter data despite the fact that we have used more basis functions and model terms for tracking the former signal. Figures 5a and 5b shows representative reconstruction of BP and pulse oximeter signals using up to 20 and 15 most significant model terms. For both signals, excellent estimates are found when they were reconstructed with more than 10 model terms. Table 1

**FIGURE 4. Representative blood pressure (BP) (top panel) and pulse oximeter (bottom panel) signals (solid lines) with estimated waveforms (dotted lines).**

shows the averaged NMSE values for the TVSINCOS, TIV, and TVAR methods for both BP and pulse oximeter data. Similar to the simulation example, the TVSINCOS significantly outperforms the other two methods for both signals. This is expected since BP dynamics are more complicated than pulse oximeter recordings (e.g., a dicrotic notch).

Respiratory Rate Detection

Table 3 shows the estimated mean respiratory rates (0.2–0.6 Hz) and the corresponding SD and error values using our algorithm. We obtained good estimation for all breathing frequencies although the estimation errors were greater for higher breathing rates. Note that a spectrum of pulse oximeter data contains more significant power at lower than higher frequencies. Thus, higher breathing rates result in more estimation errors since the algorithm has to account for inherent dynamics at lower frequencies which may have as strong magnitudes as those of a high-frequency respiratory rate.

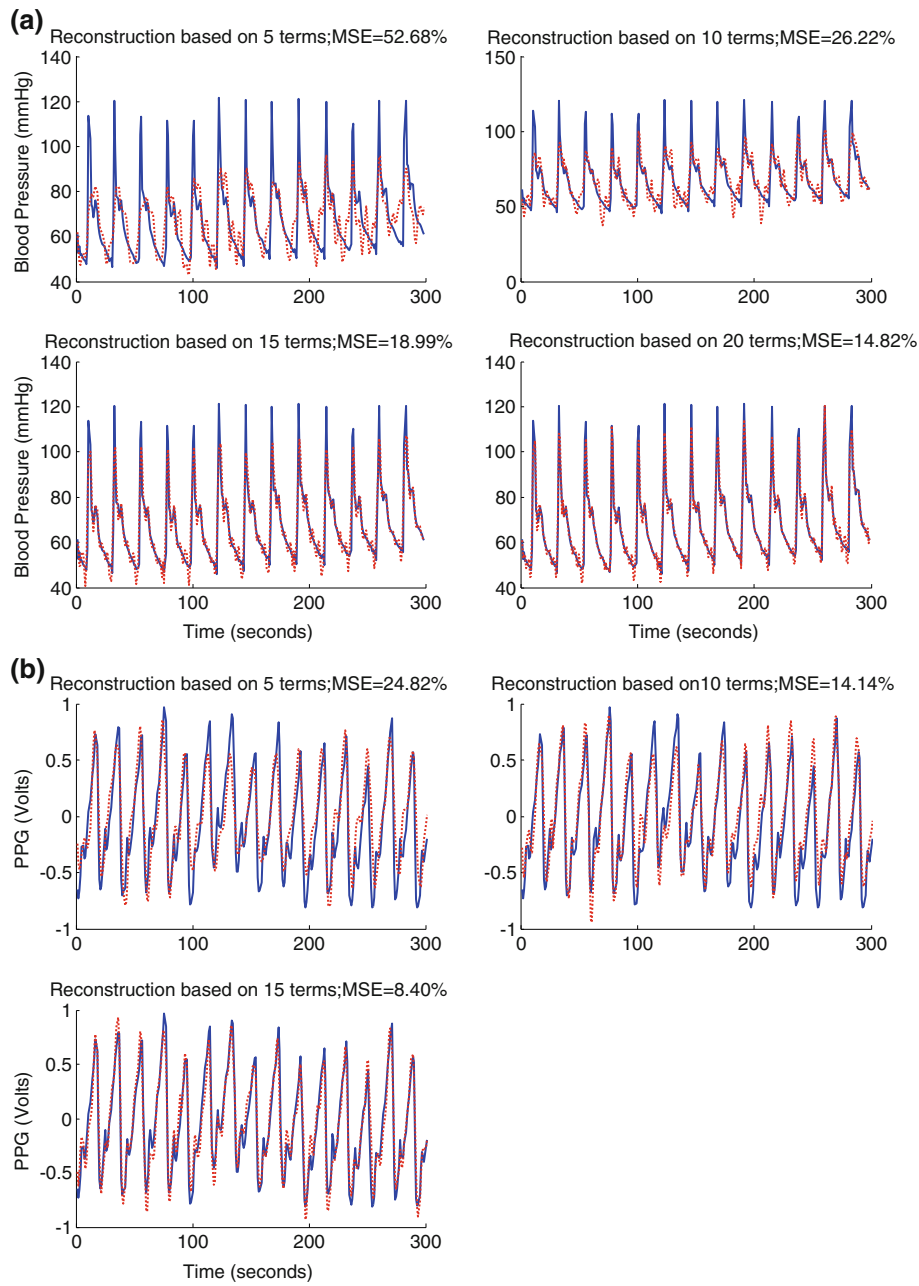


FIGURE 5. Representative reconstruction of (a): blood pressure (BP) and (b): photoplethysmogram (PPG) signals using up to 20 and 15 most significant model terms, respectively.

TABLE 3. Estimated respiratory rates and the corresponding estimation errors.

True respiratory rate (Hz)	Estimated respiratory rate (Hz)	Estimation error (%)
0.2	0.200 ± 0.000	0.00
0.3	0.297 ± 0.013	1.042
0.4	0.388 ± 0.089	3.125
0.5	0.472 ± 0.109	5.625
0.6	0.559 ± 0.104	6.771

Discussion and Conclusion

In this study, we developed a general-purpose algorithm that is especially well-suited for capturing TV periodic oscillations. The algorithm utilizes sinusoidal basis functions to model periodic oscillations and their TV properties are accounted for by using both Legendre and Walsh basis functions. We use both Legendre and Walsh basis functions to account for both slow and fast dynamics that might be present in a

signal. We have shown that employing multiple sets of basis functions is a good way to account for both fast and slow TV dynamics.⁶

Most physiological signals exhibit periodic sinusoidal oscillations. Some examples include BP, pulse oximeter, and respiratory signals, to name a few. For signals such as these, rather than using a traditional AR model-based approach, it is our opinion that the use of the sinusoids as basis functions is more appropriate. As shown in Fig. 4, we obtain good tracking capability with the proposed method for both BP and pulse oximeter data; the estimation errors were only 14 and 5% for the former and latter signals, respectively. The BP data have more complicated dynamics (e.g., the presence of dicrotic notch) than do pulse oximeter data, thus, the presence of higher estimation error was to be expected. The evidence of TV dynamics in these data is compelling as there was a further reduction of 40% in the estimation error by using a TV approach, over the TIV approach, for example, in the BP data.

It should be noted that by using the basis function approach, we significantly reduced the number of parameters that are needed to capture TV dynamics. The traditional AR model-based approaches to tracking TV systems, the recursive least squares (RLS), least mean squares (LMS), and Kalman filters, all require a significantly larger number of parameters than does a basis functions approach.^{10,28,29}

Our determination of the proper number of basis functions was based on the NMSE values among various combinations and we selected basis sets which provided the smallest error. We have previously shown that this is the most proper approach given the fact that we do not have *a priori* information on the optimal number of basis functions.²⁹ It is our experience that initially there is a sequential decrease in the NMSE values with increased number of basis sets but an excessively large number of basis sets can often lead to a dramatic increase in the NMSE values.²⁹ Our final selection of the basis sets based on the averaged NMSE value appears to be nearly optimal since there was no statistical difference between testing and training data, as shown in Table 1.

As demonstrated in this work, our proposed method works well for signals that exhibit sinusoidal oscillatory characteristics such as those examined in this work. However, for signals that do not exhibit such sinusoidal oscillatory patterns, certainly the traditional AR model-based approaches may be more appropriate. It should be noted that by exploiting the sinusoidal oscillations of the signals examined in this work, we have significantly reduced the number of parameters that are needed to capture the essential dynamics. TV AR methods that rely on LMS, RLS, or Kalman filters all require many AR parameters to capture the

dynamics at each time point, thus these methods essentially become fitting techniques. On the contrary, because our method uses a basis functions approach by exploiting *a priori* knowledge of sinusoidal patterns of the signal, we are able to drastically reduce the number of parameters required to fit the data. The significance of this is that there is a promise that even more compact model representations of the system dynamics can be developed. The models can then be utilized to be predictive and diagnostic resources for various pathological signals.

Another application of our approach was to extract respiratory rates directly from pulse oximeter recordings. Our approach was found to be accurate in detecting varying respiratory rates which ranged from 0.2 to 0.6 Hz. The estimation error was negligible at low breathing rates but increased to 7% for 36 breaths/min. This increased respiratory rate detection error may arise for the following four reasons. First, at high breathing rates, subjects had more difficulty in maintaining the desired breathing rates. Second, the subjects had to sustain lower respiratory volume for each breath which essentially resulted in lower signal-to-noise ratios. Third, there were more motion artifacts with higher breathing rates. Finally, higher breathing rates resulted in more estimation errors since the algorithm had to account for the inherent dynamics at lower frequencies which may have as strong magnitudes as those of a respiratory rate at high frequencies. Note that dynamics at lower frequencies have been attributed to the autonomic nervous system.²⁵

There has been considerable interest in extracting respiratory rates from a pulse oximeter because it would allow one additional vital sign to be obtained from the ubiquitous pulse oximeter. From the perspective of patient comfort, it is also a welcome advance since wearing an obtrusive thermister or inductance-based chest and abdomen belt (Ambulatory Monitoring Inc., Ardsley, NY) is no longer necessary.

Many different approaches have been proposed to obtain respiratory rates from pulse oximeter recordings.^{7,8,11,14,18,21,22} With the recent introduction of new techniques using estimation of time–frequency spectra for analyzing nonstationary signals, several studies have utilized short-time Fourier transform (STFT)^{24,25} and continuous wavelet transform (CWT)^{1,8,16–18} to extract the respiratory rate from the PPG signals. However, success is predicated on obtaining the highest possible time and frequency resolution, which is impossible with either the STFT or the CWT. In our recent study, we have used one of the highest time–frequency spectral techniques known as the variable frequency complex demodulation (VFCDM) approach to obtain accurate estimation of respiratory rates directly from pulse oximeter recordings.⁷ Specifically,

the VFCDM is used to extract either frequency modulation (FM) or amplitude modulation (AM) at the heart rate frequency.²⁶ The FM or AM time series is then subjected to the power spectral analysis and the largest peak in the spectrum is selected as the respiratory rate.⁷ Performance comparison was also made between VFCDM and CWT, and it was found that the former method provided better results than the latter.

Recently, a method based on AR modeling has also been proposed to extract respiratory rates.¹¹ However, it was found that the AR modeling technique was not as accurate as the VFCDM approach in obtaining respiratory rates because it relied on an inefficient model order search criterion.⁴ We are currently working on improving AR model-based approaches to obtain more robust estimates of respiratory rates that can span from as low as 6 breaths/min to as high as 90 breaths/min.

In addition to providing accurate estimation of respiratory rates, our current method provides the additional capability to track the dynamics of pulse oximeter signals. This is important because if the tracking capability deviates significantly, such an event may signify a certain abnormal condition a subject may be experiencing at that particular moment in time. During this abnormal condition, it is also likely that a subject's breathing may be significantly altered, thus having both the tracking capability and the respiratory rate information may provide more accurate diagnosis of a sudden physiological change a subject may experience. For example, in CSR, often seen in subjects with congestive heart failure, the respiratory rate suddenly stops, and then normal respiratory patterns resume.¹³ Such a complicated pattern is important to detect as it has been shown to lead to increased mortality.² In summary, we developed a TV parametric model based on sinusoids to account for the periodic oscillations of the specific physiological signals considered in our work, followed by employment of multiple sets of basis functions for the purpose of tracking both slow and sudden changes in dynamics. An additional feature of our method is that it can also provide a relatively good estimate of the breathing rates which can be combined with its tracking capability to provide more accurate diagnostic capabilities.

REFERENCES

- ¹Addison, P. S., and J. N. Watson. Secondary wavelet feature decoupling (SWFD) and its use in detecting patient respiration from the photoplethysmogram. In: Engineering in Medicine and Biology Society. Proceedings of the 25th Annual International Conference of the IEEE, 2003, Vol. 3, pp. 2602–2605.
- ²Arena, R., J. Myers, J. Abella, M. A. Peberdy, D. Bensimhon, P. Chase, and M. Gauzzi. Development of a ventilation classification system in patients with heart failure. *Circulation* 115:2410–2417, 2007.
- ³Bailon, R., L. Sornmo, and P. Laguna. A robust method for ECG-based estimation of the respiratory frequency during stress testing. *IEEE Trans. Biomed. Eng.* 53(7): 1273–1285, 2006.
- ⁴Chon, K. H., and S. Lu. A new algorithm for autoregression moving average model parameter estimation using group method of data handling. *Ann. Biomed. Eng.* 29(1): 92–98, 2001.
- ⁵Chon, K. H., M. J. Korenberg, and N. H. Holstein-Rathlou. Application of fast orthogonal search to linear and nonlinear stochastic systems. *Ann. Biomed. Eng.* 25(5): 793–801, 1997.
- ⁶Chon, K. H., H. Zhao, R. Zou, and K. Ju. Multiple time-varying dynamic analysis using multiple sets of basis functions. *IEEE Trans. Biomed. Eng.* 52(5):956–960, 2005.
- ⁷Chon, K. H., S. Dash, and K. Ju. Estimation of respiratory rate from photoplethysmogram data using time-frequency spectral estimation. *IEEE Trans. Biomed. Eng.* 56(8):2054–2063, 2009.
- ⁸Clifton, D., J. Douglas, P. Addison, and J. Watson. Measurement of respiratory rate from the photoplethysmogram in chest clinic patients. *J. Clin. Monit. Comput.* 21(1):55–61, 2007.
- ⁹Curzi-Dascalova, L., R. Flores-Guevara, S. Guidasci, G. Korn, and N. Monod. Respiratory frequency during sleep in siblings of sudden infant death syndrome victims. A comparison with control, normal infants. *Early Hum. Dev.* 8(3–4):235–241, 1983.
- ¹⁰Faes, L., H. Zhao, K. H. Chon, and G. Nollo. Time-varying surrogate data to assess nonlinearity in non-stationary time series: application to heart rate variability. *IEEE Trans. Biomed. Eng.* 56(3):685–695, 2009.
- ¹¹Fleming, S. G., and L. Tarassenko. A comparison of signal processing techniques for the extraction of breathing rate from the photoplethysmogram. *Int. J. Biomed. Sci.* 2(4):232–236, 2007.
- ¹²Francis, D. P., K. Willson, L. C. Davies, A. J. Coats, and M. Piepoli. Quantitative general theory for periodic breathing in chronic heart failure and its clinical implications. *Circulation* 102(18):2214–2221, 2000.
- ¹³Garde, A., L. Sornmo, R. Jane, and B. Giraldo. Correntropy-based spectral characterization of respiratory patterns in patients with chronic heart failure. *IEEE Trans. Biomed. Eng.*, in press, Epub 2010 March 5.
- ¹⁴Johansson, A., P. A. Oberg, and G. Sedin. Monitoring of heart and respiratory rates in newborn infants using a new photoplethysmographic technique. *J. Clin. Monit. Comput.* 15(7–8):461–467, 1999.
- ¹⁵Lee, J., and K. H. Chon. Respiratory rate extraction via an autoregressive model using the optimal parameter search criterion. *Ann. Biomed. Eng.*, in press, Epub 2010 May 25.
- ¹⁶Leonard, P., T. F. Beattie, P. S. Addison, and J. N. Watson. Standard pulse oximeters can be used to monitor respiratory rate. *Emerg. Med. J.* 20(6):524–525, 2003.
- ¹⁷Leonard, P., N. R. Grubb, P. S. Addison, D. Clifton, and J. N. Watson. An algorithm for the detection of individual breaths from the pulse oximeter waveform. *J. Clin. Monit. Comput.* 18(5–6):309–312, 2004.
- ¹⁸Leonard, P. A., D. Clifton, P. S. Addison, J. N. Watson, and T. Beattie. An automated algorithm for determining

- respiratory rate by photoplethysmogram in children. *Acta Paediatr.* 95(9):1124–1128, 2006.
- ¹⁹Lu, S., K. H. Ju, and K. H. Chon. A new algorithm for linear and nonlinear ARMA model parameter estimation using affine geometry. *IEEE Trans. Biomed. Eng.* 48(10): 1116–1124, 2001.
- ²⁰Marple Jr., S. L. *Digital Spectral Analysis*. Englewood Cliffs: Prentice Hall, 1987.
- ²¹Nakajima, K., T. Tamura, and H. Miike. Monitoring of heart and respiratory rates by photoplethysmography using a digital filtering technique. *Med. Eng. Phys.* 18(5):365–372, 1996.
- ²²Nilsson, L., A. Johansson, and S. Kalman. Respiration can be monitored by photoplethysmography with high sensitivity and specificity regardless of anaesthesia and ventilatory mode. *Acta Anaesthesiol. Scand.* 49(8):1157–1162, 2005.
- ²³Parati, G., R. Casadei, A. Groppelli, M. Di Rienzo, and G. Mancia. Comparison of finger and intra-arterial blood pressure monitoring at rest and during laboratory testing. *Hypertension* 13(6 Pt 1):647–655, 1989.
- ²⁴Shelley, K. H., R. G. Stout, and D. G. Silverman. The use of joint time frequency analysis of the pulse oximeter waveform to measure the respiratory rate of ventilated patients. *Anesthesiology* 91(3A):A583, 1999.
- ²⁵Shelley, K., A. Awad, R. Stout, and D. Silverman. The use of joint time frequency analysis to quantify the effect of ventilation on the pulse oximeter waveform. *J. Clin. Monit. Comput.* 20(2):81–87, 2006.
- ²⁶Wang, H., K. Siu, K. Ju, and K. H. Chon. A high resolution approach to estimating time-frequency spectra and their amplitudes. *Ann. Biomed. Eng.* 34(2):326–338, 2006.
- ²⁷Zhao, H., K. Ju, and K. H. Chon. An approach to estimate time-varying casual coherence function. *Methods Inf. Med.* 46(2):102–109, 2007.
- ²⁸Zou, R., and K. H. Chon. Robust algorithm for estimation of time-varying transfer functions. *IEEE Trans. Biomed. Eng.* 51(2):219–228, 2004.
- ²⁹Zou, R., H. Wang, and K. H. Chon. A robust time-varying identification algorithm using basis functions. *Ann. Biomed. Eng.* 31(7):840–853, 2003.